Cell, Vol. 81, 245–252, April 21, 1995, Copyright © 1995 by Cell Press

Impairment of Motor Coordination, Purkinje Cell Synapse Formation, and Cerebellar Long-Term Depression in GluRδ2 Mutant Mice

Nobuko Kashiwabuchi,[1]* Kazutaka Ikeda,[1]* Kazuaki Araki,[1]* Tomoo Hirano,[2] Katsuei Shibuki,[3] Chitoshi Takayama,[4] Yoshiro Inoue,[4] Tatsuya Kutsuwada,[1] Takeshi Yagi,[5,7] Youngnam Kang,[2] Shinichi Aizawa,[5,8] and Masayoshi Mishina[1,6]

[1]Department of Neuropharmacology
[3]Department of Physiology
Brain Research Institute
Niigata University
Niigata 951
Japan
[2]Department of Physiology
Kyoto University Faculty of Medicine
Kyoto 606
Japan
[4]Department of Anatomy
Hokkaido University School of Medicine
Sapporo 060
Japan
[5]Laboratory of Molecular Oncology
Tsukuba Life Science Center Institute of Physical and Chemical Research
Ibaraki 305
Japan
[6]Department of Pharmacology
University of Tokyo Faculty of Medicine
Tokyo 113
Japan

Summary

Of the six glutamate receptor (GluR) channel subunit families identified by molecular cloning, five have been shown to constitute either the AMPA, kainate, or NMDA receptor channel, whereas the function of the δ subunit family remains unknown. The selective localization of the δ2 subunit of the GluRδ subfamily in cerebellar Purkinje cells prompted us to examine its possible physiological roles by the gene targeting technique. Analyses of the GluRδ2 mutant mice reveal that the δ2 subunit plays important roles in motor coordination, formation of parallel fiber-Purkinje cell synapses and climbing fiber-Purkinje cell synapses, and long-term depression of parallel fiber-Purkinje cell synaptic transmission. These results suggest a close relationship between synaptic plasticity and synapse formation in the cerebellum.

Introduction

The glutamate receptor (GluR) channel mediates most of the fast excitatory synaptic transmission in the vertebrate central nervous system (Mayer and Westbrook, 1987) and is essential for synaptic plasticity, which is thought to underlie development, learning, and memory (Ito, 1989; McDonald and Johnston, 1990; Bliss and Collingridge, 1993). Molecular cloning has revealed a number of GluR channel subunits, which can be classified into six subfamilies according to their amino acid sequence identity (for reviews, see Mishina et al., 1993; Seeburg, 1993; Hollmann and Heinemann, 1994; Nakanishi and Masu, 1994). The α (GluR1–4), β (GluR5–7), γ (KA), ε (NR2), and ζ (NR1) subunit families have been shown by functional expression studies to constitute the GluR channel selective for either α-amino-3-hydroxy-5-methyl-4-isoxazole-propionate (AMPA), kainate, or N-methyl-D-aspartate (NMDA). We have found the δ subunit family by successive screening of mouse brain cDNA libraries (Yamazaki et al., 1992) and, with respect to the amino acid sequence identity, the δ subunit family positions in between the NMDA and non-NMDA receptor channel subunits (Yamazaki et al., 1992; Araki et al., 1993; Lomeli et al., 1993). Thus far, no GluR channel functions have been detected after expression of the δ subunit cDNAs in Xenopus oocytes or mammalian cells (Araki et al., 1993; Lomeli et al., 1993). Based on the selective localization of the δ2 subunit in cerebellar Purkinje cells, we have speculated that GluRδ2 might be involved in Purkinje cell–specific functions, such as cerebellar long-term depression (LTD) (Araki et al., 1993). To examine the possible physiological roles of the δ2 subunit, we have employed the gene targeting technique (Capecchi, 1989). Here, we show that mice defective in the GluR channel δ2 subunit are ataxic and have defects in Purkinje cell synapse formation and cerebellar LTD. Studies with primary cultures and antisense oligonucleotides have also suggested the involvement of the δ2 subunit in the cerebellar LTD (Hirano et al., 1994).

Results

Mice Defective in the GluR Channel δ2 Subunit

To disrupt the GluRδ2 locus in murine embryonic stem cells by homologous recombination, we constructed a targeting vector containing a 12 kb GluRδ2 genomic DNA fragment in which the exon encoding putative transmembrane segment M3 was replaced by a neomycin phosphotransferase gene (Figure 1A). A diphtheria toxin A fragment gene was linked to the mutated GluRδ2 gene for negative selection (Yagi et al., 1993a). The targeting vector was transfected into TT2 embryonic stem cells (Yagi et al., 1993b), and five targeted clones were identified by G418 selection, polymerase chain reaction (PCR), and Southern blot hybridization, the frequency of homologous recombination being 0.5% of G418-resistant clones. Cells of three clones were injected into 8-cell embryos of ICR

*These authors contributed equally to this work.

[7]Present address: Laboratory of Neurobiology and Behavioral Genetics, National Institute for Physiological Sciences, Okazaki 444, Japan.
[8]Present address: Laboratory of Morphogenesis, Institute of Molecular Embryology and Genetics, Kumamoto University School of Medicine, Kumamoto 860, Japan.

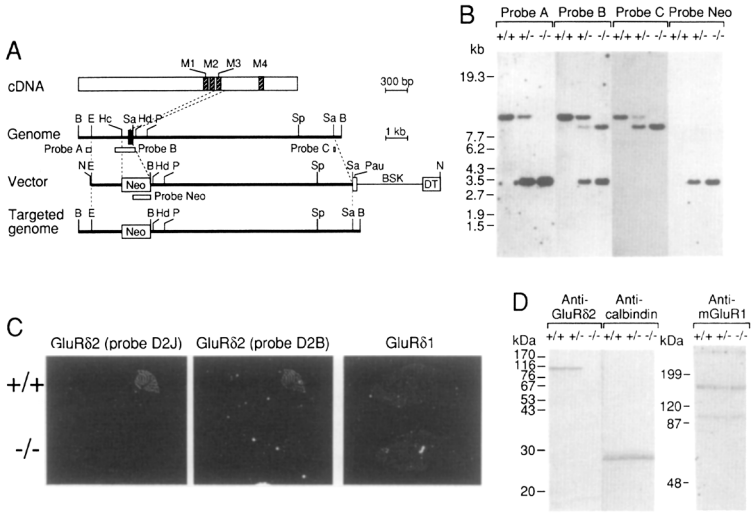

Figure 1. Targeted Disruption of the Mouse GluR Channel δ2 Subunit Gene

(A) Schematic representations of GluRδ2 cDNA, genomic DNA, targeting vector, and disrupted gene. M1–M4, four putative transmembrane segments; Neo, neomycin-resistant gene; Pau, mRNA destabilizing and transcription pausing signals; BSK, plasmid pBluescript; DT, diphtheria toxin gene; B, BamHI; E, EcoRI; Hc, HincII; Hd, HindIII; N, NotI; P, PmaCI; Sa, SacI; Sp, SpeI.

(B) Southern blot analysis of BamHI-digested genomic DNA.

(C) In situ hybridization analysis of parasagittal brain sections.

(D) Western blot analysis of cerebellar proteins with antibodies against GluRδ2, calbindin, and mGluR1.

mice to produce chimeras. Chimeras were mated to C57BL/6 mice, and those derived from clones L143 and M32 transmitted the mutation through the germline. Heterozygous progenies were intercrossed, and the offspring were analyzed by Southern blot hybridization (Figure 1B). GluRδ2 mutant mice homozygous for the disrupted GluRδ2 allele (−/−) were viable and fertile, though the mating efficiency was low.

In situ hybridization analyses of the parasagittal brain sections with an oligonucleotide probe corresponding to the disrupted region (probe D2J) showed that normal GluRδ2 RNA transcripts were absent in the mutant mice (Figure 1C). The transcripts from the disrupted GluRδ2 gene were detected with an oligonucleotide probe corresponding to the intact region (probe D2B), but their amounts were much lower than those of the normal GluRδ2 mRNA in the wild-type mice. The expression of the GluRδ1 mRNA was not appreciably affected by the GluRδ2 mutation. Western blot analysis of total cerebellar proteins showed that the mutant mice (−/−) had no detectable GluRδ2 protein, and the content of the protein of the heterozygous mice (+/−) was approximately half of the wild-type mice (+/+), whereas the contents of calbindin (Yamakuni et al., 1984), a marker protein of cerebellar Purkinje cells, and mGluR1 metabotropic GluR (Masu et al., 1991; Shigemoto et al., 1994) were not appreciably affected by the GluRδ2 mutation (Figure 1D).

Motor Coordination

The GluRδ2 mutant mice showed moderate locomotor ataxia, which could be noticed already at approximately postnatal day 12 (P12). The mutant mice often walked with tottering steps and sometimes scrambled to their hindlimbs. The spontaneous activities of the wild-type and mutant mice at P26–P28 were recorded in a computerized activity-tracing chamber, which used infrared photobeams to monitor horizontal and vertical movements (Figure 2). The mutant mice showed significantly reduced horizontal activity measured as total walking distances as compared with the wild-type mice (t test, $p < .01$). There also was a significant difference in total running time with high speeds (>20 cm/s) between the wild-type and mutant mice (t test, $p < .01$). The vertical activity typically consisted of rearing or standing up on their hindlimbs. When rearing, the mutant mice often pitched and rolled, owing to their poor balance. Total rearing time of the mutant mice was significantly shorter than that of the wild-type mice (t test, $p < .01$).

We then applied two motor tasks, the rope climbing and running along an elevated runway tasks, that were successfully used to assess quantitatively the deficits in motor performance of the *lurcher* mutant mice with defects in cerebellar Purkinje cells (Goldowitz et al., 1992). In the rope climbing task, mice were placed at the base of a suspended piece of 50 cm twine with knots at ~15 mm intervals, and the time required to climb to the top was recorded with a stopwatch. Mice at P21 were given four trials per day for 5 consecutive days. The mutant and wild-type mice climbed the twine with comparable speeds on the first two days (Figure 3C). On the last 3 days, the

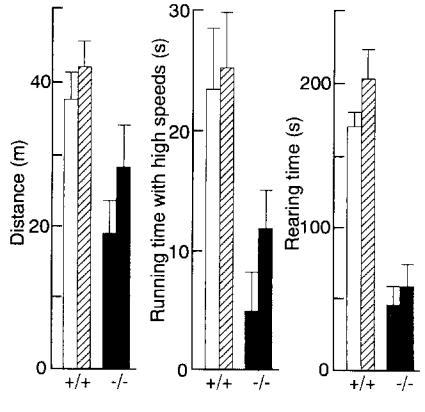

Figure 2. Locomotor Activities of the Wild-Type and Mutant Mice

Wild-type mice are indicated by (+/+); mutant mice are indicated by (−/−). Mice from lines L143 (open and closed bars) and M32 (hatched bars) were measured for 30 min in daytime using a behavioral tracing analyzer (Model BTA-I, Muromachi Kikai, Tokyo); L143 (+/+), n = 9; L143 (−/−), n = 8; M32 (+/+), n = 10; M32 (−/−), n = 11.

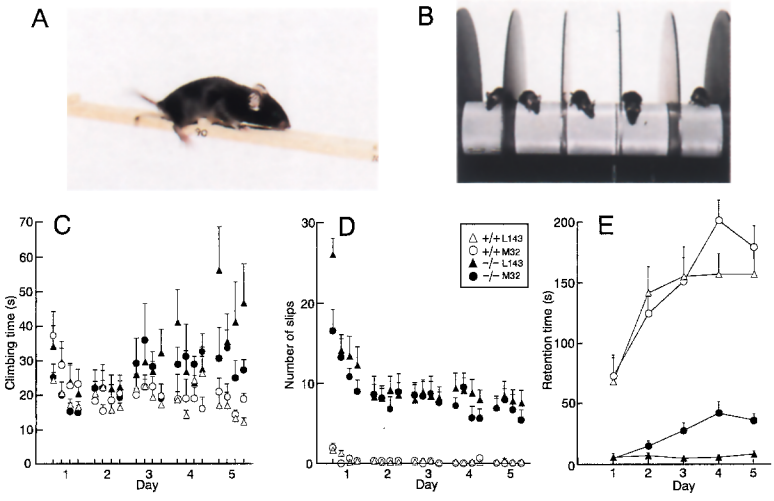

Figure 3. Behavioral Characterization of the GluRδ2 Mutant Mice

(A and D) The runway task. Number of slips was counted during walking 100 cm on a runway; L143 (+/+), n = 13; L143 (−/−), n = 13; M32 (+/+), n = 3; M32 (−/−), n = 10.

(B and E) The rotating rod task. The test was carried out for 5 min using Rota-Rod Treadmill (Muromachi Kikai, Tokyo). Retention time on the rotating rod at 10 rpm was counted; L143 (+/+), n = 9; L143 (−/−), n = 8; M32 (+/+), n = 13; M32 (−/−), n = 9.

(C) The rope climbing task. Time required for climbing 50 cm along a vertically suspended twine was measured with a stopwatch; L143 (+/+), n = 9; L143 (−/−), n = 6; M32 (+/+), n = 4; M32 (−/−), n = 3.

mutant mice took a somewhat longer time, though it was not very significant.

In the runway task (Goldowitz et al., 1992), mice run along an elevated runway with low obstacles intended to impede the progress of mice (Figure 3A). The runway was 100 cm long and 2 cm wide, about the shoulder width of a mouse, and at this width, the digits of the hindfoot usually hung over the runway edge, so a slight lateral misstep would result in a slip. The number of slips was counted during each trial. Mice at P21 were given four trials per day for 5 consecutive days. There was a clear difference in the number of slips between the wild-type and mutant mice (Figure 3D). The wild-type mice quickly ran through with few slips, except for the first day. In contrast, the mutant mice walked slowly along the runway with many slips, although an improvement was observed on the first day.

We employed the rotating rod task to further compare the motor coordination ability (Dunham and Miya, 1957). Mice at P21 were placed onto a rod of 87 mm in diameter, and the rod was rotated at 10 rpm (Figure 3B). The retention time of mice on the rod was automatically recorded (Figure 3E). Ten trials per day were given for 5 consecutive days. The wild-type mice quickly learned to retain themselves on the rod. On the other hand, the retention time of the mutant mice was much shorter than that of the wild-type mice, though an improvement was observed; only a few of L143 line showed improvements, and there may have been some differences between two lines. These results suggest that the GluRδ2 mutant mice are impaired in motor coordination, which is in accordance with the selective localization of the δ2 subunit in cerebellar Purkinje cells.

Histology

Figure 4 shows the anatomical organization of the cerebella of the wild-type and mutant mice at P28. The cerebellum of the mutant mice showed apparently normal histological appearance (Figures 4A and 4E). In Nissl-stained sections, no significant abnormality was observed in the development of the folium, the organization of the molecular, Purkinje cell, and granule cell layers, and the numbers, shapes, and distributions of neuronal and glial cells (Figures 4B and 4F). As shown by immunohistochemistry with anti-inositol trisphosphate receptor (IP_3R) antibody, Purkinje cells of the mutant mice had well-differentiated dendritic arbors, and the dendrites were studded with spines as numerous as the wild-type mice (Figures 4C and 4G).

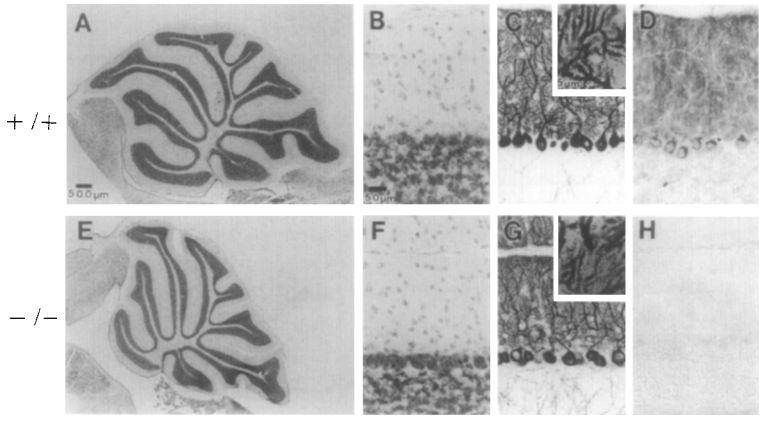

Figure 4. Histological and Immunohistochemical Analyses of Wild-Type and Mutant Cerebella

(A–D) Wild-type cerebella; (E–H) mutant cerebella.

(A and E) Nissl-stained sagittal sections of the cerebellar vermis.

(B and F) Higher magnification of (A) and (E) at the culmen.

(C and G) Cerebellar cortex immunostained with anti-IP_3R antibody. Insets show dendritic shafts and spines of Purkinje cells.

(D and H) Cerebellar cortex immunostained with anti-GluRδ2 antibody.

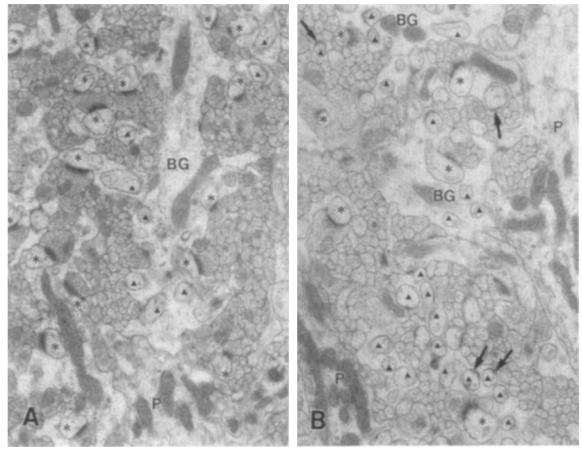

Figure 5. Electron Microscopic Analysis of the Wild-Type and Mutant Purkinje Cell Synapses

(A) Wild-type and (B) mutant Purkinje cell synapses. Asterisks, dendritic spines of the Purkinje cells with synaptic terminals; triangles, dendritic spines without synaptic terminals; arrows, high electron density in dendritic spines without synaptic terminals; BG, the processes of Bergmann glial cells; P, the dendritic shafts of Purkinje cells.

GluRδ2 immunostaining was found in the molecular and Purkinje cell layers of the wild-type cerebellum as described (Araki et al., 1993), but was abolished in the mutant cerebellum (Figures 4D and 4H).

Further inspection with electron microscopy, however, revealed an anatomical difference between the wild-type and mutant mice. Synaptic contacts with postsynaptic densities were sparse on the dendritic spines of the mutant Purkinje cells (Figure 5, asterisks). The numbers of synapses on the dendritic spines per 100 μm^2 counted on electron microscopy photographs were 16.6 ± 3.6 (mean ± SEM; n = 20) and 22.0 ± 4.5 (n = 19) for two wild-type mice, and 7.1 ± 1.6 (n = 20) and 9.9 ± 2.3 (n = 20) for two mutant mice, respectively (difference between the wild-type and mutant mice, t test, $p < .01$). Correspondingly, spines without synaptic contacts but surrounded by sheets of Bergmann glial cells were found more abundantly in the mutant mice than in the wild-type mice (Figure 5B, triangles). Some of these spines possessed high electron density, like postsynaptic membranes, but missed the synaptic contact with parallel fibers (PFs; Figure 5B, arrows). These observations suggest that the formation or maintenance of PF–Purkinje cell synapses is disturbed in the mutant mice.

Purkinje Cell Responses

Cerebellar Purkinje cells receive two distinct excitatory inputs, one from PFs and the other from climbing fibers (CFs). Voltage responses to PF and CF stimulation were measured under blind-patch recording of Purkinje cell dendrites in cerebellar slices (Shibuki and Okada, 1992). Both responses were not affected by 50 μM D-2-amino-5-phosphonovarelate, but were virtually eliminated by 10 μM 6-cyano-7-nitroquinoxaline-2,3-dion, in accordance with the previous observations (Konnerth et al., 1990; Perkel et al., 1990; data not shown). The rising slopes of

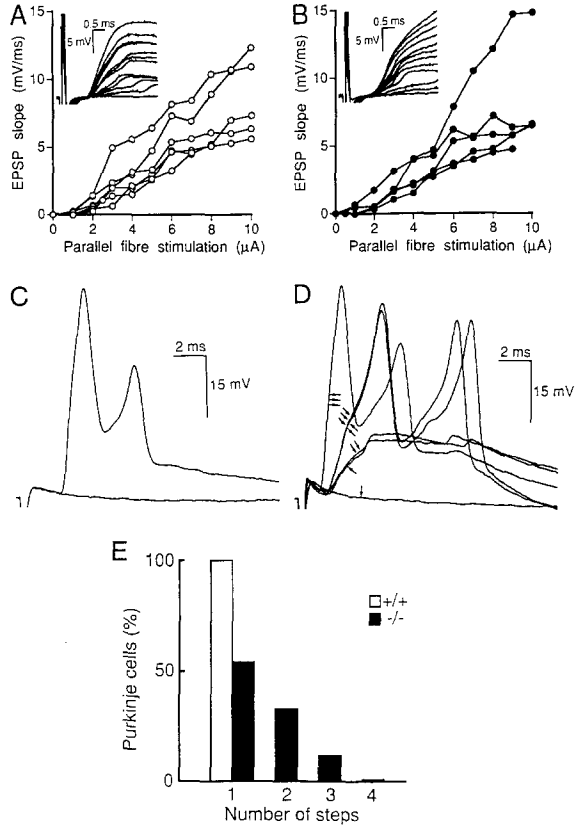

Figure 6. Voltage Responses of Purkinje Cells

(A and B) Changes in PF stimulation-evoked EPSPs in the wild-type (A) and mutant (B) Purkinje cells as increasing stimulus intensities at 0.5 or 1 μA steps. Insets show the EPSP traces.

(C and D) White matter stimulation-evoked CF responses of the wild-type (C) and mutant (D) Purkinje cells. Two traces each were recorded at the threshold intensities of 3 μA (C) or of 9, 15, and 17 μA indicated by one, two, and three arrowheads, respectively (D).

(E) Number of steps of CF EPSP of the wild-type (open bar) and mutant (closed bars) Purkinje cells.

PF stimulation-evoked excitatory postsynaptic potentials (EPSPs) gradually increased depending on the stimulus intensities, and no clear difference was observed in the slope-intensity relationships between the wild-type and mutant Purkinje cells (Figures 6A and 6B). CF responses of the wild-type Purkinje cells appeared at the threshold intensity of stimulation, and the rising EPSP slope was constant at larger stimulus intensities (n = 40 from 11 mice; Figure 6C), in accordance with innervation of a single CF to one Purkinje cell in adult animals (Crepel, 1982). In contrast, CF responses in 39 out of 85 mutant Purkinje cells (22 mice) changed in a step-wise manner at stimulus intensities larger than the threshold (Figure 6D). The rising slopes of the responses were constant between the steps. From the number of distinctive steps in CF responses, 33%, 12%, and 1% of Purkinje cells from the mutant mice were estimated to be innervated by at least two, three, and four CFs, respectively (Figure 6E). Thus, we conclude that Purkinje cells in the mutant mice remain to be multiply innervated by CFs even at the adult stage.

The excitatory synaptic transmissions on Purkinje cell

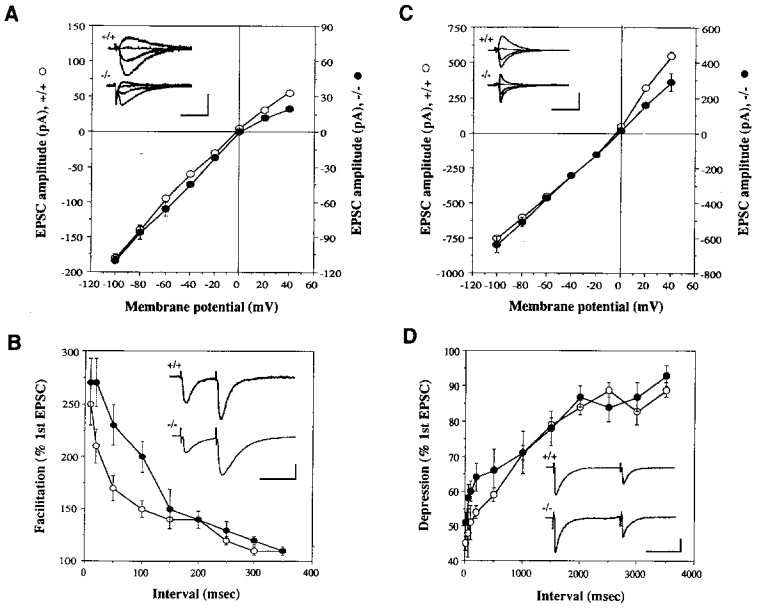

Figure 7. Current–Voltage Relations and Paired-Pulse Modulations of EPSCs in the Wild-Type and Mutant Purkinje Cells

Open circles, wild-type Purkinje cells; closed circles, mutant Purkinje cells.

(A and C) Current–voltage relations of PF EPSCs (A) and CF EPSCs (C). Each point represents mean ± SEM of 5 (A) and 2–3 (C) consecutive EPSCs evoked at 0.2 (A) and 0.1 (C) Hz. Insets show representative single PF EPSCs recorded at the holding potentials of −80 mV, −40 mV, 0 mV, and 40 mV. Bars, 20 ms and 100 pA (A); 20 ms and 500 pA (C).

(B and D) Paired-pulse facilitation of PF EPSCs (B; [+/+], n = 6 cells; [−/−], n = 7 cells) and paired-pulse depression of CF-EPSCs (D; [+/+], n = 3 cells; [−/−], n = 4 cells). The amplitude of second EPSC (expressed as percentage of the first EPSC, mean ± SEM) is plotted against interstimulus intervals. Stimulus pairs were applied at 0.2 (B) and 0.1 (D) Hz. Bars, 50 ms and 100 pA (B); 50 ms and 500 pA (+/+) or 200 pA (−/−) (C).

were further characterized by the thin slice whole-cell patch-clamp technique (Konnerth et al., 1990). There was no significant difference in the time courses of PF stimulation-induced excitatory post synaptic currents (EPSCs) between the wild-type and mutant slices. Time to peak and half-height width were 5 ± 0.5 ms and 16 ± 2.4 ms (n = 7) for the wild-type cells, and 5 ± 0.4 ms and 16 ± 1.5 ms (n = 12) for the mutant cells, respectively. The current–voltage relations of PF responses were similar between the two types of the cells (Figure 7A). The reversal potential was −1 ± 1 mV (n = 3) for the wild-type cells and −1 ± 1 mV (n = 5) for the mutant cells. No significant difference was found in the time courses of CF stimulation-induced EPSCs between the wild-type and mutant slices. Time to peak and half-height width were 1 ± 0.4 ms and 8 ± 1.2 ms (n = 3) for the wild-type cells and 1 ± 0.2 ms and 7 ± 2.7 ms (n = 5) for the mutant cells, respectively. The current–voltage relationships of CF responses were similar (Figure 7C). The reversal potential was −2 ± 1 mV (n = 3) for the wild-type cells and 1 ± 2 mV (n = 4) for the mutant cells.

As reported by Konnerth et al. (1990), the PF and CF responses exhibited paired-pulse facilitation and depression, respectively (Figures 7B and 7D). The extent of paired-pulse facilitation of PF stimulation-induced EPSCs and that of paired-pulse depression of CF stimulation-induced EPSCs were not significantly different between the wild-type and mutant Purkinje cells, except for the facilitation at the interval of 100 ms (t test, $p < .05$).

Cerebellar LTD

Coactivation of CF and PF inputs at low frequency induces LTD of the synaptic transmission between PFs and Purkinje cells, which has been considered as a cellular basis of motor learning (Ito, 1989; Linden, 1994). We employed the thin slice whole-cell patch-clamp technique to examine the cerebellar LTD in the mutant mice. With this method, Konnerth et al. (1992) showed in rats that simultaneous activation of the CFs and PFs innervating single Purkinje cells caused a LTD of transmission of the PF–Purkinje cell excitatory synapse, and the CF stimulation could be replaced by brief depolarization of Purkinje cells. Pairing of brief depolarization of the wild-type Purkinje cells with PF stimulation gradually decreased PF stimulation-induced EPSCs after strong transient depression in 12 out of 16 cells, the extent of reduction at 30 min after stimulation being 32% ± 5% (n = 16 from 10 mice; Figures 8A and 8C). However, the extent of reduction was significantly smaller in the mutant Purkinje cells (5% ± 3%; n = 21 from 10 mice; t test, $p < .01$), although the strong transient depression was always observed (Figures 8B and 8C). Of 21 mutant cells, 18 exhibited little depression, and 3 cells showed moderate depression. Thus, cerebellar LTD is impaired in the mutant mice.

Voltage-gated Ca^{2+} currents, which are required for the induction of LTD (Hirano, 1990; Sakurai, 1990; Crepel and Jaillard, 1991), were similar in amplitudes and current–voltage relations between the wild-type and mutant Purkinje cells (data not shown). The peak current amplitudes were 1.72 ± 0.64 nA (n = 5) and 1.45 ± 0.55 nA (n = 7) for the wild-type and mutant cells, respectively. The most negative potential at which the current was activated, the potential at which the peak amplitude attained one-half of the maximum value, and the potential at which the peak amplitude attained the maximum value were −52 ± 3 mV, −32 ± 2 mV, and −19 ± 2 mV for the wild-type cells (n = 5), and were −55 ± 3 mV, −28 ± 2 mV, and −16 ± 2 mV for the mutant cells (n = 7), respectively.

Discussion

In the present investigation, we have provided experimental evidence by gene targeting that the δ2 subunit of the GluR channel plays important physiological roles in vivo. Deprivation of the δ2 subunit results in disturbance of mo-

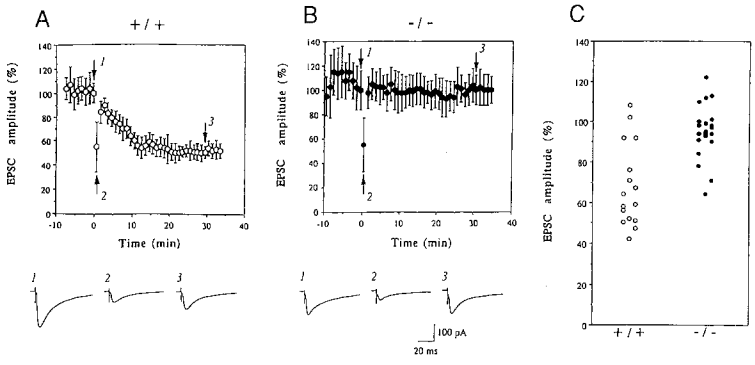

Figure 8. LTD in the Wild-Type and Mutant Cerebellar Thin Slices

(A and B) Time course of EPSC amplitudes of the wild-type (A) and mutant (B) Purkinje cells. The EPSC was evoked by stimulating PFs at 1 Hz throughout experiments. At time 0, depolarization to 0 mV for 50 ms was applied 10 times in conjunction with the PF stimulation; onset of depolarization preceded by 10 ms. Each point indicates mean ± SD of peak amplitudes of EPSCs in a 1 min bin. Lower traces are averages of 10 individual EPSCs recorded just before (1), just after (2), and 30 min after (3) the depolarization.

(C) The EPSC amplitude change in each experiment normalized by dividing the mean peak amplitude between 25 and 30 min after depolarization by the mean between 5 and 0 min before depolarization.

tor coordination, synapse formations between the PFs and Purkinje cells and between the CFs and Purkinje cells, and LTD of PF–Purkinje cell synaptic transmission in the mutant mice. The involvement of the δ2 subunit in the cerbellar LTD is in agreement with in vitro studies using cerebellar primary cultures and antisense oligonucleotides (Hirano et al., 1994).

Because available evidence suggests that the δ2 subunit is selectively localized in cerebellar Purkinje cells (Araki et al., 1993; Lomeli et al., 1993), the motor coordination deficiency of the GluRδ2 mutant mice should be ascribed primarily to the dysfunction of the mutant Purkinje cells lacking the δ2 subunit. It is possible that the δ2 subunit function may be pleiotropic, and thus the subunit would play roles independently in the formation of PF–Purkinje cell synapses, the formation of CF–Purkinje cell synapses, and the cerebellar LTD. Alternatively, there may be one primary function of the δ2 subunit, and this defect could cause the other secondary phenotypes. Since oligonucleotides antisense to the GluRδ2 mRNA suppress LTD (Hirano et al., 1994) when added to cerebellar primary cultures, the δ2 subunit is likely to be directly involved at least in the induction of the cerebellar LTD. It is known that during the normal course of development of the rodent cerebellum, the adult one-to-one relationship between CFs and Purkinje cells is preceded by a transient stage of multiple innervation (Crepel, 1982). However, Purkinje cells remain to be multiply innervated by CFs when the formation of PF–Purkinje cell synapse formation is hindered by X-ray irradiation or spontaneous mutations, such as *weaver*, *reeler*, and *staggerer* (Crepel, 1982). Thus, the multiple innervation of Purkinje cells by CFs in the GluRδ2 mutant mice might be due to the reduced PF–Purkinje cell synapse formation. Though the causal relationships of these phenotypes of GluRδ2 mutant mice remain to be established, our findings provide direct evidence for a close relationship between synaptic plasticity and synapse formation in the cerebellum.

The δ subunit family of the GluR channel was discovered by molecular cloning (Yamazaki et al., 1992). In contrast to the wide and weak expression of the δ1 subunit mRNA, the δ2 subunit mRNA is selectively localized in the cerebellar Purkinje cells (Araki et al., 1993; Lomeli et al., 1993). The δ2 subunit protein is expressed and distributed throughout the molecular layer, where the Purkinje cell dendrites develop, forming synapses with terminals of the PFs and CFs, as shown by immunostaining with anti-GluRδ2 antibody (Araki et al., 1993). Thus far, no evidence is available that the classical classification of the AMPA, kainate, and NMDA receptor channels can be adopted to the δ subunit family. Among diverse GluR channel subunits, the δ subunit, in view of the amino acid sequence identity, positions in between the NMDA and non-NMDA receptor channel subunits (Yamazaki et al., 1992; Araki et al., 1993; Lomeli et al., 1993). The AMPA receptor channel mediates the fast excitatory synaptic transmission in most of the central nervous system, whereas the NMDA receptor channel serves as a molecular coincidence detector to play a role in synaptic plasticity and synapse formation (Mayer and Westbrook, 1987; McDonald and Johnston, 1990; Bliss and Collingridge, 1993). Rabacchi et al. (1992) showed that chronic in vivo application of D-2-amino-5-phosphonovarelate into rat cerebellum prevented the regression of supernumerary CF synapses in Purkinje cells. In view of our findings that the δ2 subunit plays a role in synaptic plasticity and synapse formation, like the NMDA receptor channel, it would be of interest to examine whether the δ2 subunit forms a complex with any known GluR channel subunit or an unidentified novel subunit.

Since the subunits within the same GluR channel subfamily show similar functional properties (for reviews see Mishina et al., 1993; Seeburg, 1993; Hollmann and Heinemann, 1994; Nakanishi and Masu, 1994), it seems reasonable to assume that the widely distributed δ1 subunit might also play a role in synaptic plasticity and synapse formation. LTD in the hippocampus is prominent early in postnatal development (Dudek and Bear, 1993), and thus LTD in the cerebrum might also be related to synapse formation. Possible involvement of the δ1 subunit in these processes could be tested by the targeted disruption of the δ1 subunit gene.

Brain functions are based on highly organized networks of many neurons. The formation of specific connections among nerve cells includes innervation, preferential sur-

vival, and elimination of synapses. The δ2 subunit–deficient mutant mice will provide an excellent model system to investigate the molecular mechanisms underlying the Purkinje cell synapse formation, the cerebellar LTD, the motor learning, and their relationships.

Experimental Procedures

Production of GluRδ2 Mutant Mice

Genomic DNA from C57BL/6 mice liver was digested by BamHI, size-fractionated by 10%–38% sucrose density gradient centrifugation, and inserted into EMBL3 phage vector (Stratagene). Screening of the genomic library with the 1.3 kb HindIII–BamHI fragment from pA37–31 (Araki et al., 1993) yielded clone λD2–9. The 12 kb genomic DNA insert containing 140 bp exon encompassing putative transmembrane segment M3 of the δ2 subunit and the 2.0 kb EcoRI–HindIII fragment from the insert were cloned into pBluescript II KS$^-$ to yield pD2–9 and pD2–9EH, respectively. The 4.5 kb HincII–SacI fragment from pD2–9EH and the 1.3 kb EcoRI–BamHI fragment from pGK2Neo (Yagi et al., 1993a) were blunted and ligated to yield pD2–9Neo. The 2.4 kb HindIII fragment from pD2–9 was inserted into the HindIII site of pD2–9Neo to yield pD2–9NeoH. The 25 bp NotI–XhoI segment of pPauDT1 (Sakimura, K. et al., 1995) was replaced by synthetic linker

5′-GGCCGCCACGTGGAGCTCC-3′
3′-CGGTGCACCTCGAGGAGCT-5′

to yield pPauDT2. The 3.3 kb NotI–PmaCI fragment from pD2–9NeoH, the 6.9 kb PmaCI–SpeI and 1.5 kb SpeI–SacI fragments from pD2–9, and the 4.0 kb SacI–NotI fragment from pPauDT2 were ligated to yield pTVGRδ2.

TT2 embryonic stem cells (Yagi et al., 1993b) were transfected by NotI-cleaved pTVGRδ2, and GluRδ2 mutant mice were produced and housed as described (Hogan et al., 1986; Nada et al., 1993). In situ hybridization analyses were carried out as described (Watanabe et al., 1992). Oligonuceotide probes D1A, D2B, and D2J are complementary to the nucleotide residues 2907–2951 of the δ1 subunit cDNA (Yamazaki et al., 1992) and 2901–2945 and 1818–1862 of the δ2 subunit cDNA (Araki et al., 1993), respectively. Western blot analyses were carried out as described (Araki et al., 1993), except that mGluR1 protein was visualized by enhanced chemiluminescence (Amersham). Anti-calbindin and anti-mGluR1 antibodies were provided by Dr. T. Yamakuni and Dr. S. Nakanishi, respectively.

Histology

The sagittal sections of 20 μm in thickness were prepared from mice at P28 by a cryostat for Toluidine blue staining and immunohistochemistry with anti-IP_3R monoclonal antibody $_4C_{11}$ (provided by Dr. K. Mikoshiba) or anti-GluRδ2 antibody by ABC method (Hsu et al., 1981). For detailed observation of dendritic spines of Purkinje cells, the sections of 100 μm in thickness cut by a microslicer (DSK-1000, Dosaka, Kyoto) were immunostained with $_4C_{11}$ and were osmicated for enhancement of diaminobenzidine reaction. The sections were embedded within flattened epoxy resin.

Mice at P28 were perfused with 0.1 M phosphate buffer (pH 7.4) containing 4% paraformaldehyde and 0.5% glutaraldehyde. Sagittal blocks of the cerebellum postfixed with 1% osmium were embedded within epoxy resin. Ultrathin sections of the culmen were double-stained with 1% uranyl acetate and mixed lead solution. For quantitative measurements, the molecular layer of the cerebellum at the two-fifths depth from pial side was selected. Number of synapses on the dendritic spines was counted on photographs at a final magnification of 12,000×.

Electrophysiology

Parasagittal slices (400 μm thick) of the cerebellar vermis were prepared from mice at P28 to P44. Intracellular voltage recording from Purkinje cell dendrites within 100 μm from the cut surface of slices (Shibuki and Okada, 1992) was done at 30°C by a blind-patch recording technique with glass micropipettes of 12–34 MΩ filled with a medium containing 140 mM potassium methanesulphonate, 10 mM KCl, 10 mM HEPES (adjusted to pH 7.2 with KOH), 1 mM disodium citrate, 2 mM Na_2–ATP, 0.3 mM GTP, and 50 mM glucose. External perfusing medium contained 124 mM NaCl, 5 mM KCl, 1.24 mM NaH_2PO_4, 1.3 mM $MgSO_4$, 2.4 mM $CaCl_2$, 10 mM glucose, and 26 mM $NaHCO_3$ saturated with 95% O_2 and 5% CO_2. The resting membrane potential was −53 to −40 mV, and the input resistance was 20–70 MΩ. PFs were stimulated every 12 s by a biphasic pulse (duration, 200 μs; intensity, ± 0.5 to ± 10 μA) through a glass micropipette filled with 2 M NaCl and 1% or saturated Fast Green FCF, which was inserted into the molecular layer 300 μm below the surface. CFs were stimulated by a monophasic pulse (duration, 300 μs; intensity, 13–30 μA) through a Teflon-coated platinum wire of 75 μm diameter placed on the white matter. Stimulating pulse intensities were limited to diminish possible effects of inhibitory interneurons.

The thin slice patch-clamp recording was carried out essentially as described (Konnerth et al., 1992). Transverse slices (200 μm) cut from the cerebellum of mice at P14–P22 were perfused continuously at 22°C–24°C with an external solution saturated with 95% O_2 and 5% CO_2 in the presence of 20 μM bicuculline; for Ca^{2+} current measurements, slices were prepared from mice at P5–P8. A cell body of Purkinje neuron was whole-cell voltage clamped at −80 mV with a patch pipette of 3–4 MΩ. Input resistance (100–300 MΩ) and series resistance (20–40 MΩ) were monitored by applying 80 ms voltage pulse to −90 mV every 5 min, and experiments were terminated when these values changed more than 20%. A patch pipette filled with the external solution was positioned about 100 μm away from the recorded cell body and was used to stimulate PFs in the molecular layer. CF was stimulated by placing the stimulation electrode in the vicinity of the Purkinje cell body. The EPSC evoked by the CF was identified by its large amplitude and its all-or-none characteristic; with threshold stimulus, the response was either full amplitude or zero. The intracellular solution contained 140 mM CsCl, 0.5 mM EGTA, and 10 mM HEPES (pH 7.3); 2 mM MgATP and 0.3 mM GTP were added for the LTD experiments and Ca^{2+} current measurements. The external solution contained 124 mM NaCl, 26 mM $NaHCO_3$, 1.8 mM KCl, 1.24 mM KH_2PO_4, 2.5 mM $CaCl_2$, 1.3 mM $MgCl_2$, and 10 mM glucose. Recorded current was filtered at 10 kHz, stored in a DAT recorder (TEAC, RD-130TE), and analyzed off-line.

Acknowledgments

We thank Mr. N. Takeda for help in the preparation of chimeric mice, Dr. T. Yamakuni for anti-calbindin antibody, Dr. S. Nakanishi for anti-mGluR1 antibody, Dr. K. Mikoshiba for anti-IP_3R antibody, and Drs. M. Ito, H. Niki, and M. Kano for critical reading of the manuscript. This investigation was supported by research grants from the Ministry of Education, Science, and Culture of Japan, the Institute of Physical and Chemical Research, the Ministry of Health and Welfare of Japan, the Uehara Memorial Foundation, and the Yamanouchi Foundation.

Received October 19, 1994; revised January 31, 1995.

References

Araki, K., Meguro, H., Kushiya, E., Takayama, C., Inoue, Y., and Mishina, M. (1993). Selective expression of the glutamate receptor channel δ2 subunit in cerebellar Purkinje cells. Biochem. Biophys. Res. Commun. *197*, 1267–1276.

Bliss, T. V. P., and Collingridge, G. L. (1993). A synaptic model of memory: long-term potentiation in the hippocampus. Nature *361*, 31–39.

Capecchi, M. R. (1989). Altering the genome by homologous recombination. Science *244*, 1288–1292.

Crepel, F. (1982). Regression of functional synapses in the immature mammalian cerebellum. Trends Neurosci. *5*, 266–269.

Crepel, F., and Jaillard, D. (1991). Pairing of pre- and postsynaptic activities in cerebellar Purkinje cells induces long-term changes in synaptic efficacy in vitro. J. Physiol. *432*, 123–141.

Dudek, S. M., and Bear, M. F. (1993). Bidirectional long-term modification of synaptic effectiveness in the adult and immature hippocampus. J. Neurosci. *13*, 2910–2918.

Dunham, N. W., and Miya, T. S. (1957). A note on a simple apparatus for detecting neurological deficit in rats and mice. J. Am. Pharm. Assoc. *46*, 208–209.

Goldowitz, D., Moran, T. H., and Wetts, R. (1992). Mouse chimeras in the study of genetic and structural determinants of behavior. In Techniques for the Genetic Analysis of Brain and Behavior, D. Goldowitz, D. Wahlsten, and R. E. Wimer, eds. (Amsterdam: Elsevier), pp. 271–290.

Hirano, T. (1990). Effects of postsynaptic depolarization in the induction of synaptic depression between a granule cell and a Purkinje cell in rat cerebellar culture. Neurosci. Lett. *119*, 145–147.

Hirano, T., Kasono, K., Araki, K., Shinozuka, K., and Mishina, M. (1994). Involvement of the glutamate receptor δ2 subunit in the long-term depression of glutamate responsiveness in cultured rat Purkinje cells. Neurosci. Lett. *182*, 172–176.

Hogan, B., Costantini, F., and Lacy, E. (1986). Manipulating the Mouse Embryo: A Laboratory Manual. (Cold Spring Harbor, New York: Cold Spring Harbor Laboratory Press).

Hollmann, M., and Heinemann, S. (1994). Cloned glutamate receptors. Annu. Rev. Neurosci. *17*, 31–108.

Hsu, S.-M., Raine, L., and Fanger, H. (1981). Use of avidin-biotin-peroxidase complex (ABC) in immunoperoxidase techniques: a comparison between ABC and unlabeled antibody (PAP) procedures. J. Histochem. Cytochem. *29*, 577–580.

Ito, M. (1989). Long-term depression. Annu. Rev. Neurosci. *12*, 85–102.

Konnerth, A., Llano, I., and Armstrong, C. M. (1990). Synaptic currents in cerebellar Purkinje cells. Proc. Natl. Acad. Sci. USA *87*, 2662–2665.

Konnerth, A., Dreessen, J., and Augustine, G. J. (1992). Brief dendritic calcium signals initiate long-lasting synaptic depression in cerebellar Purkinje cells. Proc. Natl. Acad. Sci. USA *89*, 7051–7055.

Linden, D. J. (1994). Long-term synaptic depression in the mammalian brain. Neuron *12*, 457–472.

Lomeli, H., Sprengel, R., Laurie, D. J., Köhr, G., Herb, A., Seeburg, P. H., and Wisden, W. (1993). The rat delta-1 and delta-2 subunits extend the excitatory amino acid receptor family. FEBS Lett. *315*, 318–322.

Masu, M., Tanabe, Y., Tsuchida, K., Shigemoto, R., and Nakanishi, S. (1991). Sequence and expression of a metabotropic glutamate receptor. Nature *349*, 760–765.

Mayer, M. L., and Westbrook, G. L. (1987). The physiology of excitatory amino acids in the vertebrate central nervous system. Prog. Neurobiol. *28*, 197–276.

McDonald, J. W., and Johnston, M. V. (1990). Physiological and pathophysiological roles of excitatory amino acids during central nervous system development. Brain Res. Rev. *15*, 41–70.

Mishina, M., Mori, H., Araki, K., Kushiya, E., Meguro, H., Kutsuwada, T., Kashiwabuchi, N., Ikeda, K., Nagasawa, M., Yamazaki, M., Masaki, H., Yamakura, T., Morita, T., and Sakimura, K. (1993). Molecular and functional diversity of the NMDA receptor channel. Ann. NY Acad. Sci. *707*, 136–152.

Nada, S., Yagi, T., Takeda, H., Tokunaga, T., Nakagawa, H., Ikawa, Y., Okada, M., and Aizawa, S. (1993). Constitutive activation of Src family kinases in mouse embryos that lack Csk. Cell *73*, 1125–1135.

Nakanishi, S., and Masu, M. (1994). Molecular diversity and functions of glutamate receptors. Annu. Rev. Biophys. Biomol. Struct. *23*, 319–348.

Perkel, D. J., Hestrin, S., Sah, P., and Nicoll, R. A. (1990). Excitatory synaptic currents in Purkinje cells. Proc. R. Soc. Lond. (B) *241*, 116–121.

Rabacchi, S., Bailly, Y., Delhaye-Bouchaud, N., and Mariani, J. (1992). Involvement of the N-methyl-D-aspartate (NMDA) receptor in synapse elimination during cerebellar development. Science *256*, 1823–1825.

Sakimura, K., Kutsuwada, T., Ito, I., Manabe, T., Takayama, C., Kushiya, E., Yagi, T., Aizawa, S., Inoue, Y., Sugiyama, H., and Mishina, M. (1995). Reduced hippocampal LTP and spatial learning in mice lacking NMDA receptor ε1 subunit. Nature *373*, 151–155.

Sakurai, M. (1990). Calcium is an intracellular mediator of the climbing fiber in induction of cerebellar long-term depression. Proc. Natl. Acad. Sci. USA *87*, 3383–3385.

Seeburg, P. H. (1993). The molecular biology of mammalian glutamate receptor channels. Trends Neurosci. *16*, 359–365.

Shibuki, K., and Okada, D. (1992). Cerebellar long-term potentiation under suppressed postsynaptic Ca^{2+} activity. Neuroreport *3*, 231–234.

Shigemoto, R., Abe, T., Nomura, S., Nakanishi, S., and Hirano, T. (1994). Antibodies inactivating mGluR1 metabotropic glutamate receptor block long-term depression in cultured Purkinje cells. Neuron *12*, 1245–1255.

Watanabe, M., Inoue, Y., Sakimura, K., and Mishina, M. (1992). Developmental changes in distribution of NMDA receptor channel subunit mRNAs. Neuroreport *3*, 1138–1140.

Yagi, T., Nada, S., Watanabe, N., Tamemoto, H., Kohmura, N., Ikawa, Y., and Aizawa, S. (1993a). A novel negative selection for homologous recombinants using diphtheria toxin A fragment gene. Anal. Biochem. *214*, 77–86.

Yagi, T., Tokunaga, T., Furuta, Y., Nada, S., Yoshida, M., Tsukada, T., Saga, Y., Takeda, N., Ikawa, Y., and Aizawa, S. (1993b). A novel ES cell line, TT2, with high germline-differentiating potency. Anal. Biochem. *214*, 70–76.

Yamakuni, T., Usui, H., Iwanaga, T., Kondo, H., Odani, S., and Takahashi, Y. (1984). Isolation and immunohistochemical localization of a cerebellar protein. Neurosci. Lett. *45*, 235–240.

Yamazaki, M., Araki, K., Shibata, A., and Mishina, M. (1992). Molecular cloning of a cDNA encoding a novel member of the mouse glutamate receptor channel family. Biochem. Biophys. Res. Commun. *183*, 886–892.